Carbohydrate Polymers 83 (2011) 966–972

Contents lists available at ScienceDirect

Carbohydrate Polymers

journal homepage: www.elsevier.com/locate/carbpol

Cellulose/graphite oxide composite films with improved mechanical properties over a wide range of temperature

Donglin Han[a,b], Lifeng Yan[a,b,*], Wufeng Chen[a,b], Wan Li[a,b], P.R. Bangal[c]

[a] Hefei National Laboratory for Physical Sciences at the Microscale, and Anhui Province Key Laboratory of Biomass Clean Energy, University of Science and Technology of China, Hefei 230026, PR China
[b] Department of Chemical Physics, University of Science and Technology of China, Hefei 230026, PR China
[c] Inorganic and Physical Chemistry Division, Indian Institute of Chemical Technology, Tarnaka, Hyderabad 500607, India

ARTICLE INFO

Article history:
Received 7 July 2010
Received in revised form 10 August 2010
Accepted 5 September 2010
Available online 15 September 2010

Keywords:
Cellulose
Graphite oxide
Composite

ABSTRACT

Regenerated cellulose/graphite oxide (GO) blended films have been prepared in 6 wt.%NaOH/4 wt.%urea aqueous solution by a simple and cost effective method. The structure, thermal stability and mechanical properties of these composite films have been investigated by wide-angle X-ray diffraction, scanning electron microscopy, thermal analyses, and tensile strength measurements. The results obtained from those different studies revealed that cellulose and GO are mixed homogeneously. The thermal stability and mechanical properties of the composite materials are improved significantly over those of pure cellulose. The cellulose/GO film showed a high storage modulus up to 180 °C. The effect of the amount of GO content in the composite material has also been investigated.

1. Introduction

Bio-based materials have attracted much attention for their renewability and biodegradability (Gross & Kalra, 2002; Nishio, 2006; Ragauskas et al., 2006). Cellulose, the most affluent biopolymer resource in the world, is widely considered as an inexhaustible raw material with fascinating structures and properties. It has growing demand due to its environment friendly and biocompatible products (Klemm, Heublein, Fink, & Bohn, 2005; Klemm et al., 2006; Read & Bacic, 2002). It is well known that cellulose is the main reinforcing constituent in plant cell walls and it is a natural linear polysaccharide in which D-glucopyranose rings are connected to one another with β-(1,4)-D-glycosidic links. Here, making use of cellulose is believed to be a route to prepare materials and chemicals instead of petrochemicals (Mascal & Nikitin, 2008; Nogi & Yano, 2008). However, cellulose has not yet been used in optimum potential applications, because neither it can be melted nor it can be dissolved in a common solvent easily to fabricate into a desired form. Thus, more attention has been paid on searching suitable solvent systems for cellulose (de Menezes, Pasquini, Curvelo, & Gandini, 2009; El Seoud, Koschella, Fidale, Dorn, & Heinze, 2007; Heinze et al., 2000; McCormick, Callais, & Hutchinson, 1985; Yan & Gao, 2008; Zhang, Ruan, & Zhou, 2001; Zhu et al., 2006). It has been confirmed that cellulose could be well dissolved in the NaOH/urea aqueous solution at low temperature (Isogai & Atalla, 1998; Laszkiewicz, 1998; Zhang et al., 2001).

It is widely accepted that blending is an important method for developing novel polymeric materials of potential application. Blending cellulose with other material is an interesting approach for preparing functional composites (Liang et al., 2009; Yang et al., 2009; Yun & Kim, 2008; Zhang, Wang, Zhang, Wu, Zhang, & He, 2007). Zhang et al. reported that the blending of carbon nanotube with cellulose enhanced the mechanical properties of the composite materials (Zhang et al., 2007). Recently, organic/inorganic intercalation composites have also attracted many scientists because of their excellent physical–chemical properties (Bartholome, Derre, Roubeau, Zakri, & Poulin, 2008).

Graphene, a single layer of carbon atoms in a hexagonal lattice, has recently attracted much attention due to its novel electronic and mechanical properties (Ramanathan et al., 2008). Graphene is usually prepared by the reduction of its precursor graphite oxide (GO) (Chen, Yan, & Bangal, 2010), a typical pseudo-two-dimensional oxygen-containing solid in bulk form which possesses functional groups including hydroxyls, epoxides, and carboxyls (McAllister et al., 2007; Niyogi et al., 2006; Stankovich et al., 2007; Vickery, Patil, & Mann, 2009). Both graphene and GO papers show very high mechanical properties, and they are also the potential reinforcing materials for polymers (Stankovich et al., 2006; Wakabayashi et al., 2008; Wang, Tambraparni, Qiu, Tipton, & Dean, 2009). The chemical functionalization of GO has been found to be a feasible and effective means of improving the dispersion of graphene. Additionally, functional side groups bound to the surface

* Corresponding author at: Department of Chemical Physics, University of Science and Technology of China, Jinzai Road 96#, Hefei 230026, Anhui, PR China. Tel.: +86 551 3606853; fax: +86 551 3602969.
E-mail address: lfyan@ustc.edu.cn (L. Yan).

0144-8617/$ – see front matter © 2010 Elsevier Ltd. All rights reserved.
doi:10.1016/j.carbpol.2010.09.006

of graphene sheet may improve interfacial bonding between the graphene and the matrix similar to that observed for functionalized carbon nanotube-based composites (Coleman et al., 2004). Thus, this remarkable mechanical property of low costs, 2D graphene or GO sheets is expected to offer promising nanoscale filler for the next generation of composite materials. In other way, these functional groups allow GO to be easily absorbed in polar matrices and in polar polymers to form GO intercalated exfoliated composites. However, there are some reports pertaining to the intriguing applications (such as organic conductive films and heat-resistant material) of GO–polymer composites (Fang, Wang, Lu, Yang, & Nutt, 2009; Kong, Yoo, & Jung, 2009). Since GO can be dispersed in water as the individual sheet, it is possible to achieve a truly molecular-level dispersion of GO when water is used as the common solvent for both GO and the polymer matrix. Arguably it is considered that H-bonding interaction is stronger than van der Waals interaction and it can give effective interfacial adhesion between the filler and matrix.

Taking these considerations into account, we report here a simple and environmentally friendly preparation of cellulose–GO composite films by blending GO into the microcrystalline cellulose (MCC) matrix using alkali aqueous solution as the processing solvent. The structure and morphology of these prepared films are examined and discussed. These composite films combining the advantages of the cellulose and GO, result in a high mechanical performance. Good adhesion is found between GO filler and the cellulose matrix, and significant reinforcement is observed. Furthermore, we suggest that the cellulose/GO composites have high degree of heat-resistant than that of pure regenerated cellulose (RC). In addition, the effect of the blending content of GO on the properties of the prepared composites is also systematically investigated.

2. Experimental

2.1. Materials

MCC with a purity >99% was supplied by Shanghai Chemical Fiber Co. Ltd. (Shanghai, China). Its viscosity-average molecular weight (M_η) was determined using an Ubbelohde viscometer in NaOH(6 wt.%)/urea(4 wt.%) aqueous solution at $25 \pm 0.05\,^\circ$C and calculated using the equation $[\eta] = 3.85 \times 10^{-2} M_\eta^{0.76}$ to be 7.5×10^4 g mol^{-1}.(Zhou, Zhang, & Cai, 2004).

All the reagents (urea, NaOH, $NaNO_3$, 98%H_2SO_4, 30% H_2O_2 and $KMnO_4$) of analytical grade were purchased from Sinopharm Chemical Reagent Co. Ltd. in China and were used as received without further purification. Ultrapure water with resistivity of 18 MΩ cm was produced by a Milli-Q (Millipore, USA) and was used for solution preparation. Graphite powder, natural, briquetting grade, 99.9995% (metals basis) was purchased from Alfa Aesar.

2.2. Preparation of GO

GO was prepared from natural graphite by the well-known Hummers method with little modification (Becerril et al., 2008; William, Hummers, & Richard, 1958). In brief, 2 g of the natural graphite powder was added into a 250 mL beaker, then 1 g of $NaNO_3$ and 46 mL of H_2SO_4 were added into it sequentially under stirring in an ice-bath. Next, 6 g of $KMnO_4$ was added slowly into the beaker under stirring and the temperature was controlled up to 20 °C. The ice-bath was removed after 5 min and the system was heated at 35 °C for 30 min, and then 92 mL water was added slowly into the system and it was stirred for another 15 min. Then 80 mL hot water with 60 °C and 3% H_2O_2 aqueous solution were added to reduce the residual $KMnO_4$ till no bubble appears. Finally, the system was centrifuged at 7200 rpm for 10 min, and the product was washed by warm water until the pH value of the upper layer suspension arrives to 7. The obtained yellow-brown powder was re-dispersed into ultrapure water and was treated at ultrasonic power of 0.06 W/cm^3 for 15 min. A homogeneous suspension of different concentrations was prepared after filtering the trace black residues. GO powder was obtained after freezing drying of the suspension.

2.3. Preparation of films

Highly oxidized GO, especially the one synthesized from natural graphite, can be easily dispersed in water. However, desired amount of GO powder (0.10–0.30 g) was dispersed into 90 mL of ultrapure water and was treated at ultrasonic power of 0.06 W/cm^3 for 15 min in a 250 mL beaker, and homogeneous suspension of GO was found. These suspensions were pre-cooled to 0 °C in a refrigerator. After that, 6.0 g of NaOH and 4.0 g of urea were added into the prepared suspensions, and then 4.0 g of MCC powder was added sequentially into it under stirring in an ice-bath. After 10 min of stirring, the prepared mixtures (6 wt.%NaOH/4 wt.%urea/4 wt.%MCC/different contents of GO) were cooled to −15 °C and held at that temperature for 2 h. The resulting mixture solution was stirred at room temperature for 30 min. The mixed solution was cast on a glass plate and a gel-like sheet with a thickness of about 0.8 mm was found. Then the sheet was immediately immersed into 5 wt.% H_2SO_4 aqueous solution for 5 min to obtain composite film. The prepared films were washed by running water and dried in air at room temperature for 48 h following dried at 80 °C for 10 min. Finally, the composite films were dried in a vacuum at 30 °C for further experiment. By changing the weight ratio of MCC to GO, such as 40:1, 40:2, and 40:3, a series of RC/GO blended films were prepared and to identify the respective film a coded is given as RC/GO-1, RC/GO-2, and RC/GO-3. In particular, the film with code RC-0 was prepared from pure MCC in the NaOH/urea aqueous solution using the same method. Apparently, the content of GO in the composite films (cellulose and GO) are 0, 2.5, 5.0, and 7.5 wt.%. Since GO aggregates in higher concentration the film with more than 7.5 wt.% of GO is very difficult to prepare following the described method.

2.4. Characterization

Thermal analyses of the films were measured in air by Shimadzu TGA-50 thermogravimetric instrument. The temperature range is employed from 20 to 700 °C with a heating rate of 10 °C min^{-1}.

To observe crystal structure of the films, wide angle X-ray diffraction (XRD) measurements were performed on a setup with Mar 345 image plate as detector and the Cu Kα was used as the source (wavelength λ = 0.1542 nm). The recorded region of 2θ was from 5° to 45° with scanning speed 2.0°/min.

FTIR spectroscopy was used to obtain the information about the interactions between cellulose and GO sample. FTIR were measured on a Perkin-Elmer FTIR in the range 4000–600 cm^{-1}.

The surface morphology of the films was measured using a Shimadzu scanning electron microscopy (SEM) (Superscan SSX-550, Japan). The films were frozen in liquid nitrogen, and immediately snapped and then vacuum-dried. The fracture surface (cross-section) of the films was coated with gold, and then observed and photographed.

The tensile strength (σ_B) and elongation at break (ε_B) of the composite films were measured on a universal tensile tester (TS7104, Shenzhen SANS Test machine, China) according to ISO527-3:1995 at a speed of 5.0 mm min^{-1}. The specimens were in rectangular shape with dimension of 20 mm × 5 mm × 0.07 mm. The length between two grips was set as 10 mm. The average values and standard deviations of the Young's modulus and tensile strength σ_{max} were evaluated for five tested specimens. Dynamic mechanical

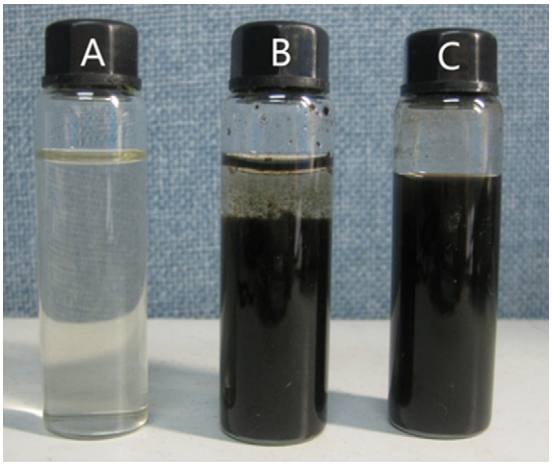

Fig. 1. Photographs of the cellulose NaOH/urea aqueous solution (A), the mixture of GO and aqueous solution of NaOH/urea (B), and the mixture of GO and cellulose in its NaOH/urea aqueous solution (C).

analysis (DMA) was conducted on a dynamic mechanical analyzer (DMA-7, Perkin-Elmer Instruments). The measurements were performed in a nitrogen atmosphere to avoid thermal oxidation. A heating rate of 5 °C min^{-1} was applied in 1 Hz frequency for an original length of 10 mm. A tensile deformation of 0.25% was applied to the specimen.

Contact angles of the films with the water were measured by a contact angle goniometry (JC2000C, Zhongcen, Shanghai, China) at room temperature.

3. Results and discussion

Fig. 1 shows the photographs of cellulose (4 wt.%) in NaOH/urea aqueous solution, GO (0.3 wt.%) in NaOH/urea aqueous solution and the mixture of GO (0.3 wt.%) and cellulose (4 wt.%) in its NaOH/urea aqueous solution, which shows the maximum stability of the systems in solution. Apparently, there easily forms aggregates of GO in the aqueous solution of NaOH/urea while there forms a stable suspension of GO in the presence of cellulose in the aqueous solution of NaOH/urea, indicates cellulose could prevent the aggregating of GO in the solution at high NaOH concentration. The as-prepared homogeneous suspension of cellulose and GO make it possible to prepare blend film of them.

The optical photographs of the pure RC film (RC-0) and the RC/GO film (RC/GO-3) are shown in Fig. 2. The thicknesses of these films are 70 ± 6 μm. The transmittance of the film RC-0 is 61.1% for 540 nm light where as the transmittance of the film RC/GO-3 is found to be only 0.83% at that wavelength.

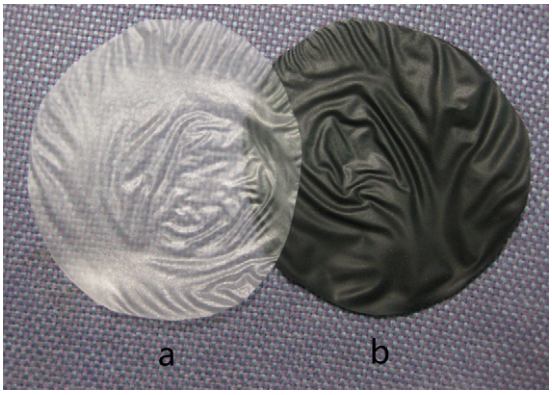

Fig. 2. The optical photographs of the RC film (a) and the RC/GO film (b).

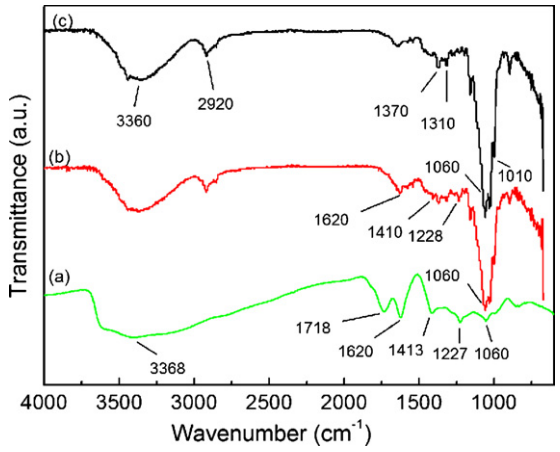

Fig. 3. XRD patterns of RC-0, RC/GO-1, RC/GO-2, RC/GO-3, and pristine GO.

The XRD patterns of the films with different GO contents are shown in Fig. 3. The interlayer spacing of our synthesized GO is 0.83 nm, which is within the range of values that have been previously reported (Bissessur, Liu, White, & Scully, 2006; Scully, Bissessur, MacLean, & Dahn, 2009). However, all other prepared films starting from RC-0 to RC/GO-3 exhibit three distinct peaks at $2\theta = 12.1°$, 19.8°, and 21.0°, which are assigned to be the $(1\bar{1}0)$, (110), and (200) planes of crystalline form of cellulose-II. The diffraction angles of the blended films are almost similar to that of the pure RC, and the diffraction peaks corresponding to GO is not observed and it could be the indication of the further exfoliation of GO into single layer during blending. In addition, the color of the composite film turned to black, which indicates the reduction of GO takes place in some extent during the preparation of the film. It is reported that GO can be reduced to graphene in the presence of aqueous NaOH (Fan et al., 2008) and we presume the similar mechanism could be operative here too and a detail study is required to explore the fact in depth and it is planned soon. However, the stronger diffraction intensity of the cellulose film than that of the cellulose/GO composite film at $2\theta = 12.1°$ implied a slightly higher crystallinity of the former than the latter. The crystallinity indexes of RC-0, RC/GO-1, RC/GO-2, and RC/GO-3 are calculated to be 51.6, 47.7, 45.5, and 44.2%. Interestingly, the crystallinity decreases on increasing the amount of GO in the composite film owing to the

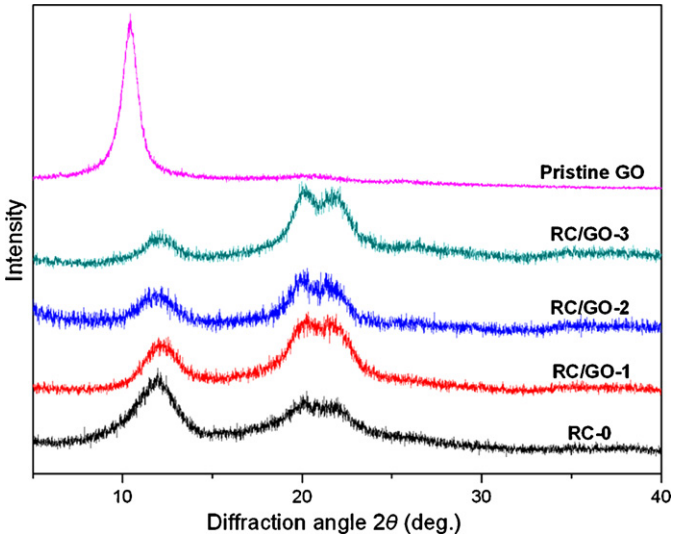

Fig. 4. The FTIR spectra for pristine GO, RC/GO-3, and RC-0.

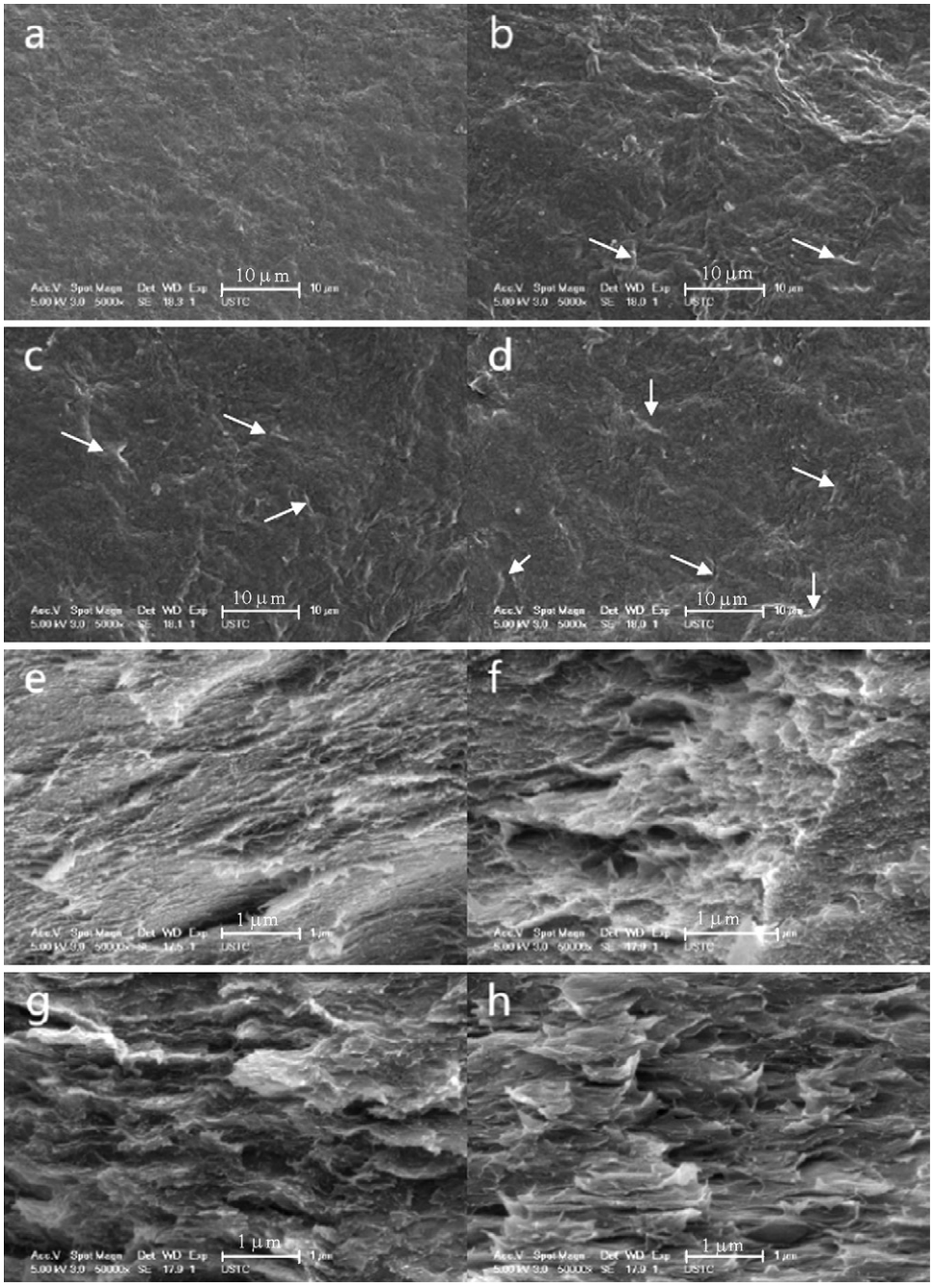

Fig. 5. SEM images of surfaces of RC-0 (a), RC/GO-1 (b), RC/GO-2 (c), and RC/GO-3 (d), and the cross-sections of RC-0 (e), RC/GO-1 (f), RC/GO-2 (g), and RC/GO-3 (h).

contribution of the amorphous state of GO. In addition, appearance of diffused intensity peaks around 19.8° indicates that the cellulose films contain considerable proportion of the amorphous region and it could be due to neutralization–coagulation. However, the structures of the cellulose in the blended films barely change, which indicates that there are mainly physical interactions between cellulose and GO, but scarcely chemical reaction between them.

FTIR studies confirm the successful oxidation of graphite to graphite oxide. The IR spectrum of our GO is similar to a previous report in the literature (Bissessur, Liu, & Scully, 2006). The FTIR spectrum of GO in Fig. 4(a) depicts a strong –OH peak at 3368 cm^{-1} and other C–O functionalities such as COOH (1718 cm^{-1}), C–OH (1413 cm^{-1}), and C–O–C (1227 cm^{-1} and 1060 cm^{-1}). The spectrum also shows a C=C peak at 1620 cm^{-1} corresponding to the remaining sp^2 character. The FTIR spectrum of RC-0 is shown in Fig. 4(c), and the diffraction curve is of typical cellulose structure. The peaks around 3360 cm^{-1} are corresponding to –OH stretching vibration (wide and strong). The peak at 2920 cm^{-1} is assigned to C–H stretching vibration. The peaks at 1010 and 1160 cm^{-1} are attributed to alcoholic group of C–OH. The peak at 1370 and 1310 cm^{-1} are assigned to C–H/CH_2 bending vibration. The peaks of the characteristic absorption in the curve of RC/GO are approximately similar with the curve of pure cellulose as shown in Fig. 4(b). However, the result indicates the formation of an intercalated and exfoliated structure. The curve of the RC/GO compound shows a combination of characteristics similar to that of the pure cellulose and GO which includes the broad absorption band located at 3360 cm^{-1} assigned to the –OH groups in GO and cellulose. The peaks at 1620, 1410, 1228 and 1060 cm^{-1} are corresponding to C=C and C–OH/C–O–C group from GO respectively, which indicates suc-

cessful blending GO with cellulose. Besides, the peak at 1718 cm^{-1} is disappeared in the curve of the RC/GO compound compared with that of pristine GO, because COOH groups from GO have been reacted with the alkaline solution in the process of preparing the films.

SEM measurements provide direct information regarding the interfacial bonding of these blended films, as shown in Fig. 5. In Fig. 5(a), the surface of the RC-0 displayed homogeneous mesh structures, which are attributed to the self-aggregation tendency of cellulose in solution and the penetration of coagulants in the coagulation process (Weng, Zhang, Ruan, Shi, & Xu, 2004). The surface of RC/GO-1, RC/GO-2, and RC/GO-3 shows smooth morphology (Fig. 5(b)–(d)) which indicate that the cellulose is miscible with GO. Due to the physical crosslinking and chain entangling of the cellulose fibers, the inner structure of RC/GO-1, RC/GO-2, and RC/GO-3 is denser than that of RC-0, and it predicts to enhance the tensile strength of composite films. In addition, surface of the blended films exhibits high level of homogeneity which indicates that the cellulose fibers and the GO fillers are completely unified in the composite and the blended films are successfully formed. The distribution of GO in the composite films is indicated by the white arrows (Fig. 5). The cross-sections of the blended films show grooves of different magnitudes due to different structures and stiffness between cellulose and GO (Fig. 5(e)–(h)). A clear stratification appeared in RC/GO-3 as the amount of exfoliated GO is very high. However, since the blending of GO is covered by a cellulose layer, there is barely a fully exfoliated GO sheet available, which indicates a good adhesion between the cellulose and the GO.

The contact angle of the pure RC-0 film with water is 12.9°, where as the contact angle of the RC/GO film with water is found to be 51.5°. This enhance of contact angle on going from RC-0 to RC/GO film not only suggests the enhancement of hydrophobicity of the blended films but also reveals that the microstructures of the RC/GO films are more compact than that of the RC-0 film. This observation nicely supports the results of SEM analysis.

The thermogravimetry (TG) and differential thermogravimetry (DTG) curves of the films are shown in Fig. 6. The T_i value is the initial decomposition temperature. T_{max} is the temperature with maximum decomposition rate, and T_f is the final decomposition temperature. For the pure cellulose film, T_i = 210 °C, T_{max} = 316 °C, and T_f = 366 °C, while for the RC/GO-3 film, T_i = 231 °C, T_{max} = 340 °C, and T_f = 391 °C. The T_{max} of the blended films are higher than that of the pure cellulose film, which indicates the involvement of strong interaction between the cellulose and GO leading to improve the thermostability of the blended films. From Fig. 6(a), it can also be seen that the char yield of the films increased by GO incorporated into the fibers. For example, at 350 °C, the char yield of pure RC film was about 40 wt.%, whereas RC/GO composite films containing 7.5 wt.% GO had char yields of about 47 wt.%. This means that the most part of GO remained in the composites at high temperature. Thus, it may be expected that cellulose composite films containing GO would possess better mechanical properties than pure cellulose films at high temperature.

The typical stress–strain (σ *vs* ε) curves for the prepared films are presented in Fig. 7. The tensile strain at the breaking point gradually increases on increasing the amount of GO into the composite film. The RC-0 film shows minimum tensile strain at the breaking point. This result combines to the fact that the addition of GO could effectively improve the mechanical strength of the film. Furthermore, with an increase of the amount of GO in the blended film from 2.5 to 7.5 wt.%, the σ_{max} values sharply jump from 54.6 ± 2.9 to 83.1 ± 3.8 MPa. This strong dependence of the tensile strength on the content of GO is perhaps due to the dispersion of GO in molecular level leading to strong H-bonding interaction between the cellulose fibers and the surface of GO.

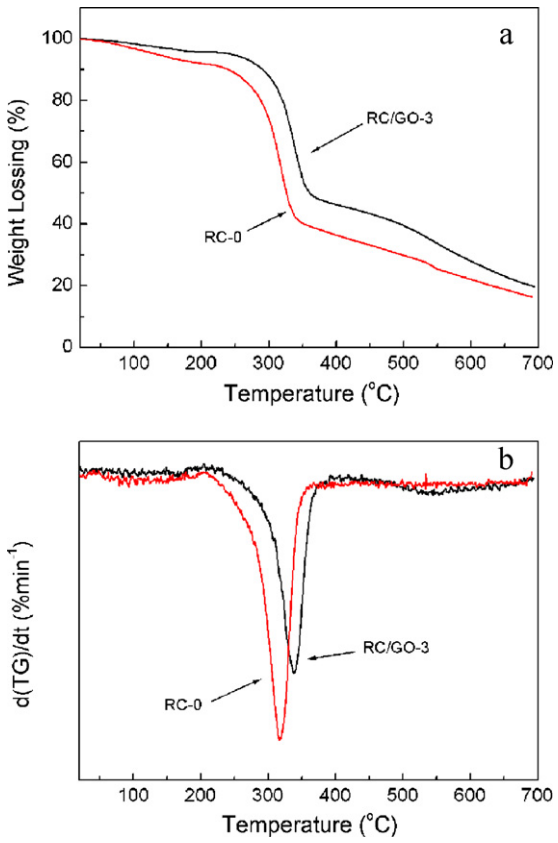

Fig. 6. TG (a) and DTG (b) curves of the films.

The Young's moduli of the films are also calculated, and they are 1.19, 1.28, 1.45, and 1.91 GPa for the RC-0, RC/GO-1, RC/GO-2, and RC/GO-3 films, respectively. For all the films, the Young's modulus increases gradually with the increase of loaded amount of GO, which indicates that the addition of GO helps to increase the interaction between the fibers.

The dynamic storage modulus E' of the films is measured by DMA as shown in Fig. 8. For the RC-0, RC/GO-1, RC/GO-2, and RC/GO-3 films the E' values are 1.39, 1.55, 1.75, and 1.99 GPa at 25 °C while they are 0.57, 1.02, 1.44, and 1.80 GPa at 180 °C, and the ratio of E'(180 °C)/E'(25 °C) are 0.41, 0.66, 0.82 and 0.90. It could be seen that the storage moduli of all the RC/GO films are higher than that of the pure RC film, and this effect is particularly more prominent at higher temperatures. In addition, it is also observed that the

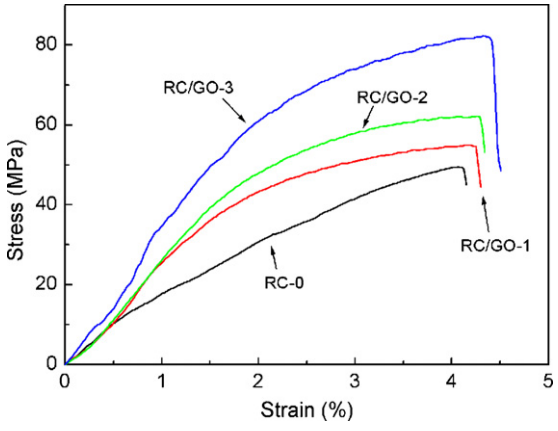

Fig. 7. Stress–strain curve of the prepared composites.

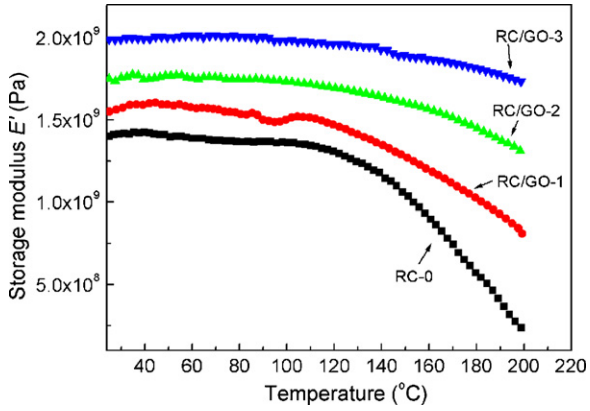

Fig. 8. Temperature dependence of the dynamic storage modulus E' of the prepared films.

higher loading of GO in the film qualitatively enabled the cellulose matrix to sustain a high modulus in higher temperature. The retention ratio, defined as the ratio of the storage modulus at 180 °C to that at 25 °C, is a measure of the mechanical properties of materials with temperature. It could be seen that the retention ratio increases on increasing the content of GO. The retention ratio is only 0.41 for the RC-0 film, but it reaches to 0.90 for the RC/GO film containing 7.5 wt.% GO. These results indicate that the RC/GO films, especially those containing more GO, possess improved mechanical properties at higher temperatures.

The data of TG/DTG and DMA above strongly suggest that the content of GO has significantly improved the thermal stability of the blended films. When the amount of GO is low in the composite, the interaction force between the GO layers and cellulose is not very high and the cellulose chain could move when heated. When the amount of GO is increased, the amount of polar groups also is increased, and the interaction force (van der Waals force and H-bonding force) between the GO layers and cellulose is enhanced resulting the restriction in the movement of cellulose chain. Hence, GO blended cellulose films can be utilized for potential high temperature application.

4. Conclusions

Blended films of cellulose and GO are successfully prepared using alkali aqueous solution as solvent. This is a simple, low cost, and "green" pathway preparing composite film of required properties. The results revealed improved thermostability and higher mechanical properties of the RC films blended with less than 7.5 wt.% GO. All the results summarize to the conclusive fact that GO is well-dispersed in the cellulose matrix, and there is strong H-bonding interaction between hydroxy groups of the cellulose and hydroxy groups of the GO. A 98% increase in tensile strength and a 60% improvement of Young's modulus are achieved by addition of only 7.5 wt.% GO. The obtained composited films own higher mechanical strength than the pure RC film, especially at high temperature. Therefore, the blended films with features of safeness, and thermostability may have promising applications in day to day life.

Acknowledgements

This work is supported by the National Natural Science Foundation of China (No. 20874095), the National Basic Research Program of China (Nos. 2007CB210201 and 2010CB923302), Chinese Universities Scientific Fund and the National Major Specific Project for Innovation of New Pharmaceuticals (No. 2009ZX09103-715).

References

Bartholome, C., Derre, A., Roubeau, O., Zakri, C., & Poulin, P. (2008). Electromechanical properties of nanotube–PVA composite actuator bimorphs. *Nanotechnology*, *19*(32), 1–6.
Becerril, H. A., Mao, J., Liu, Z., Stoltenberg, R. M., Bao, Z., & Chen, Y. (2008). Evaluation of solution-processed reduced graphene oxide films as transparent conductors. *ACS Nano*, *2*(3), 463–470.
Bissessur, R., Liu, P. K. Y., & Scully, S. F. (2006). Intercalation of polypyrrole into graphite oxide. *Synthetic Metals*, *156*(16–17), 1023–1027.
Bissessur, R., Liu, P. K. Y., White, W., & Scully, S. F. (2006). Encapsulation of polyanilines into graphite oxide. *Langmuir*, *22*(4), 1729–1734.
Chen, W. F., Yan, L. F., & Bangal, P. R. (2010). Preparation of graphene by the rapid and mild thermal reduction of graphene oxide induced by microwaves. *Carbon*, *48*(4), 1146–1152, 338.
Coleman, J. N., Cadek, M., Blake, R., Nicolosi, V., Ryan, K. P., Belton, C., et al. (2004). High-performance nanotube reinforced plastics: Understanding the mechanism of strength increase. *Advanced Functional Materials*, *14*(8), 791–798.
de Menezes, A. J., Pasquini, D., Curvelo, A. A. D., & Gandini, A. (2009). Self-reinforced composites obtained by the partial oxypropylation of cellulose fibers. 2. Effect of catalyst on the mechanical and dynamic mechanical properties. *Cellulose*, *16*(2), 239–246.
El Seoud, O. A., Koschella, A., Fidale, L. C., Dorn, S., & Heinze, T. (2007). Applications of ionic liquids in carbohydrate chemistry: A window of opportunities. *Biomacromolecules*, *8*(9), 2629–2647.
Fan, X. B., Peng, W. C., Li, Y., Li, X. Y., Wang, S. L., Zhang, G. L., et al. (2008). Deoxygenation of exfoliated graphite oxide under alkaline conditions: A green route to graphene preparation. *Advanced Materials*, *20*(23), 4490–4493.
Fang, M., Wang, K. G., Lu, H. B., Yang, Y. L., & Nutt, S. (2009). Covalent polymer functionalization of graphene nanosheets and mechanical properties of composites. *Journal of Materials Chemistry*, *19*(38), 7098–7105.
Gross, R. A., & Kalra, B. (2002). Biodegradable polymers for the environment. *Science*, *297*(5582), 803–807.
Heinze, T., Dicke, R., Koschella, A., Kull, A. H., Klohr, E. A., & Koch, W. (2000). Effective preparation of cellulose derivatives in a new simple cellulose solvent. *Macromolecular Chemistry and Physics*, *201*(6), 627–631.
Isogai, A., & Atalla, R. H. (1998). Dissolution of cellulose in aqueous NaOH solutions. *Cellulose*, *5*(4), 309–319.
Klemm, D., Heublein, B., Fink, H. P., & Bohn, A. (2005). Cellulose: Fascinating biopolymer and sustainable raw material. *Angewandte Chemie-International Edition*, *44*(22), 3358–3393.
Klemm, D., Schumann, D., Kramer, F., Hessler, N., Hornung, M., Schmauder, H. P., et al. (2006). Nanocelluloses as innovative polymers in research and application. In *Polysaccharides II*. Berlin: Springer-Verlag., pp. 49–96.
Kong, B. S., Yoo, H. W., & Jung, H. T. (2009). Electrical conductivity of graphene films with a poly(allylamine hydrochloride) supporting layer. *Langmuir*, *25*(18), 11008–11013.
Laszkiewicz, B. (1998). Solubility of bacterial cellulose and its structural properties. *Journal of Applied Polymer Science*, *67*(11), 1871–1876.
Liang, J. J., Huang, Y., Zhang, L., Wang, Y., Ma, Y. F., Guo, T. Y., et al. (2009). Molecular-level dispersion of graphene into poly(vinyl alcohol) and effective reinforcement of their nanocomposites. *Advanced Functional Materials*, *19*(14), 2297–2302.
Mascal, M., & Nikitin, E. B. (2008). Direct, high-yield conversion of cellulose into biofuel. *Angewandte Chemie-International Edition*, *47*(41), 7924–7926.
McAllister, M. J., Li, J. L., Adamson, D. H., Schniepp, H. C., Abdala, A. A., Liu, J., et al. (2007). Single sheet functionalized graphene by oxidation and thermal expansion of graphite. *Chemistry of Materials*, *19*(18), 4396–4404.
McCormick, C. L., Callais, P. A., & Hutchinson, B. H. (1985). Solution studies of cellulose in lithium-chloride and N,N-dimethylacetamide. *Macromolecules*, *18*, 2394.
Nishio, Y. (2006). Material functionalization of cellulose and related polysaccharides via diverse microcompositions. *Advances in Polymer Science*, 97–151.
Niyogi, S., Bekyarova, E., Itkis, M. E., McWilliams, J. L., Hamon, M. A., & Haddon, R. C. (2006). Solution properties of graphite and graphene. *Journal of the American Chemical Society*, *128*(24), 7720–7721.
Nogi, M., & Yano, H. (2008). Transparent nanocomposites based on cellulose produced by bacteria offer potential innovation in the electronics device industry. *Advanced Materials*, *20*(10), 1849–1852.
Ragauskas, A. J., Williams, C. K., Davison, B. H., Britovsek, G., Cairney, J., Eckert, C. A., et al. (2006). The path forward for biofuels and biomaterials. *Science*, *311*(5760), 484–489.
Ramanathan, T., Abdala, A. A., Stankovich, S., Dikin, D. A., Herrera-Alonso, M., Piner, R. D., et al. (2008). Functionalized graphene sheets for polymer nanocomposites. *Nature Nanotechnology*, *3*(6), 327–331.
Read, S. M., & Bacic, T. (2002). Plant biology—Prime time for cellulose. *Science*, *295*(5552), 59–60.
Scully, S. F., Bissessur, R., MacLean, K. W., & Dahn, D. C. (2009). Inclusion of poly[bis(methoxyethoxyethoxy)phosphazene] into layered graphite oxide. *Solid State Ionics*, *180*(2–3), 216–221.
Stankovich, S., Dikin, D. A., Dommett, G. H. B., Kohlhaas, K. M., Zimney, E. J., Stach, E. A., et al. (2006). Graphene-based composite materials. *Nature*, *442*(7100), 282–286.
Stankovich, S., Dikin, D. A., Piner, R. D., Kohlhaas, K. A., Kleinhammes, A., Jia, Y., et al. (2007). Synthesis of graphene-based nanosheets via chemical reduction of exfoliated graphite oxide. *Carbon*, *45*(7), 1558–1565.
Vickery, J. L., Patil, A. J., & Mann, S. (2009). Fabrication of graphene-polymer nanocomposites with higher-order three-dimensional architectures. *Advanced Materials*, *21*(21), 2180–2184.

Wakabayashi, K., Pierre, C., Dikin, D. A., Ruoff, R. S., Ramanathan, T., Brinson, L. C., et al. (2008). Polymer-graphite nanocomposites: Effective dispersion and major property enhancement via solid-state shear pulverization. *Macromolecules*, *41*(6), 1905–1908.

Wang, S. R., Tambraparni, M., Qiu, J. J., Tipton, J., & Dean, D. (2009). Thermal expansion of graphene composites. *Macromolecules*, *42*(14), 5251–5255.

Weng, L. H., Zhang, L. N., Ruan, D., Shi, L. H., & Xu, J. (2004). Thermal gelation of cellulose in a NaOH/thiourea aqueous solution. *Langmuir*, *20*(6), 2086–2093.

William, S., Hummers, J., & Richard, E. (1958). Preparation of graphitic oxide. *Journal of the American Chemical Society*, *80*(6), 1339–11339.

Yan, L. F., & Gao, Z. J. (2008). Dissolving of cellulose in PEG/NaOH aqueous solution. *Cellulose*, *15*(6), 789–796.

Yang, Q. L., Lue, A., Qi, H. S., Sun, Y. X., Zhang, X. Z., & Zhang, L. N. (2009). Properties and bioapplications of blended cellulose and corn protein films. *Macromolecular Bioscience*, *9*(9), 849–856.

Yun, S., & Kim, J. (2008). Characteristics and performance of functionalized MWNT blended cellulose electro-active paper actuator. *Synthetic Metals*, *158*(13), 521–526.

Zhang, L. N., Ruan, D., & Zhou, J. P. (2001). Structure and properties of regenerated cellulose films prepared from cotton linters in NaOH/urea aqueous solution. *Industrial & Engineering Chemistry Research*, *40*(25), 5923–5928.

Zhang, H., Wang, Z. G., Zhang, Z. N., Wu, J., Zhang, J., & He, H. S. (2007). Regenerated-cellulose/multiwalled-carbon-nanotube composite fibers with enhanced mechanical properties prepared with the ionic liquid 1-allyl-3-methylimidazolium chloride. *Advanced Materials*, *19*(5), 698–704.

Zhou, J. P., Zhang, L. N., & Cai, J. (2004). Behavior of cellulose in NaOH/urea aqueous solution characterized by light scattering and viscometry. *Journal of Polymer Science Part B: Polymer Physics*, *42*(2), 347–353.

Zhu, S. D., Wu, Y. X., Chen, Q. M., Yu, Z. N., Wang, C. W., Jin, S. W., et al. (2006). Dissolution of cellulose with ionic liquids and its application: A mini-review. *Green Chemistry*, *8*(4), 325–327.